CO_2 avoidance cost of fly ash geopolymer concrete

Chenchen Luan, Ao Zhou, Ye Li, Dujian Zou, Pan Gao, Tiejun Liu*

Guangdong Provincial Key Laboratory of Intelligent and Resilient Structures for Civil Engineering, Harbin Institute of Technology, Shenzhen 518055, China

* Corresponding author, liutiejun@hit.edu.cn

Abstract: Using geopolymer concrete (GC) is a technically feasible decarbonization strategy in the cement and concrete industry shown by numerous papers. A key factor determining its commercial application is whether its cost is competitive. However, related study is scarce. In this paper, we present the first analysis of GC's CO_2 avoidance cost, the cost incurred to reduce one metric ton of CO_2 emissions. The results show that out of the 486 GC mixtures analyzed, only seven yield negative CO_2 avoidance costs, while 379 are even more expensive than capturing CO_2 from cement plants, which is another technically feasible decarbonization strategy and has been evaluated to have a CO_2 avoidance cost of 55 USD/tCO_2 in China's demonstration project. Only a few GC mixtures with lower CO_2 avoidance costs will be considered for use by the industry, and they are associated with low activator dosage and high compressive strength. To quantify this relationship, we introduce the activator index (*Ai*), which refers to the activator dosage ($kg \cdot m^{-3}$) required to achieve 1 MPa of compressive strength. The result shows that *Ai* values below certain thresholds correspond to lower CO_2 avoidance costs and significant emission reductions of GC. This *Ai*-based criterion helps identify the optimal GC mixture that effectively reduces CO_2 emissions at the lowest possible cost, thereby promoting its commercial application.

Keywords: geopolymer; alkali-activated material; fly ash; cost; CO_2 emissions

1. Introduction

Approximately 8% of global CO_2 emissions and 13% of China's CO_2 emissions are attributed to Portland cement, a primary binder in concrete [1,2]. With such extensive CO_2 emissions, replacing cement with lower-carbon binders (alternative binders) to produce concrete has attracted great interest [1,3-13]. Geopolymer, also known as alkali-activated material, is identified as a promising alternative binder [6]. It is synthesized by the reaction between an alkali activator and an

aluminosilicate material (the precursor), often utilizing aluminosilicate by-products or wastes like fly ash. To date, the study on geopolymer concrete (GC)'s microstructure and engineering performances has become relatively mature [7].

While extensive studies have shown the technical feasibility of GC, limited studies are available on its economic feasibility, which limits its commercial application [4,8]. A few studies measured the cost of GC [14-17]. However, these studies have limitations: 1) They only focused on a limited number of mixtures, making the results less representative. Given the wide range of geopolymer mix designs and precursor sources, it is necessary to use a large number of mixtures to evaluate the cost and CO_2 emissions of GC [18]. 2) They used cement concrete produced using 100% ordinary Portland cement (OPC) as the reference concrete, which overestimates the carbon emission advantages of geopolymer and underestimates the cost disadvantage of geopolymer. Blended cement concrete, incorporating supplementary cementitious materials (SCMs) like fly ash to partially replace OPC, has become commercialized and standardized [19,20]. Its cost and CO_2 emissions are much lower than cement concrete using 100% OPC. It is necessary to use blended cement concrete as the reference concrete to evaluate the cost and CO_2 emissions of GC.

Even compared to cement concrete using 100% OPC, the results of McLellan et al. [14], Chan et al. [15], and Rajini et al. [16] show that GC tends to be more expensive. Currently, the damages to society caused by CO_2 emissions are borne neither by buyers nor sellers of concrete products. Hence, the industry has little motivation to use GC to replace cement concrete solely for lower CO_2 emissions if the cost of GC is higher than cement concrete. Recognizing this market problem, many governments are contemplating the implementation of carbon pricing policies [21]. Nonetheless, GC needs to exhibit a lower CO_2 avoidance cost than other decarbonization technologies or carbon pricing to be prioritized in practical applications [22]. CO_2 avoidance cost, denoting the cost incurred to reduce one metric ton (t) of CO_2, is a critical metric for such evaluations.

Both replacing cement with geopolymer and capturing CO_2 from cement plants have the potential to significantly reduce CO_2 emissions [8], rendering them competitors. The CO_2 avoidance cost of capturing CO_2 from cement plants has been extensively studied [22-26]. Notably, the carbon capture

demonstration project of the Baimashan cement plant in Conch Cement Company, China, shows a CO_2 avoidance cost of 55 USD/tCO_2 (380 CNY/tCO_2) [27]. However, there is a lack of study on evaluating GC's CO_2 avoidance cost. Given that the technology with a lower CO_2 avoidance cost holds precedence for practical application, it is vital to evaluate GC's CO_2 avoidance cost and then compare it with capturing CO_2 from cement plants to identify the cost-optimal technology.

This study presents a calculation method for the CO_2 avoidance cost of GC. Based on the method and 486 fly ash geopolymer concrete (FAGC) mixtures, this study quantifies the CO_2 avoidance cost of FAGC in the context of locally-available materials in China and compares it with capturing CO_2 from cement plants (55 USD/tCO_2). Using locally-available materials to produce geopolymer is vital because long transport distances lead to high costs and CO_2 emissions [6]. Northwest China, with its abundant fly ash resources as the geopolymer precursor [28,29], along with rich NaCl resources [30] and a well-established chlor-alkali industry [31] for producing the activator NaOH, ensures material availability for large-scale geopolymer application. This study also identifies the critical features of geopolymer mixtures with a lower CO_2 avoidance cost. This study provides valuable new insights into the application potential of geopolymer as a sustainable alternative binder and helps identify cost-optimal decarbonization technology in the cement and concrete industry.

2. Methods

Section 2.1 describes the calculation method of the CO_2 avoidance cost of GC. It involves comparing the costs and CO_2 emissions of GC and a reference cement concrete (CC). Section 2.2 describes the calculation method of costs and CO_2 emissions of FAGC and CC. Two key issues include the estimation of energy use for heat-curing with different heating temperatures and times and CO_2 emissions allocation of fly ash based on economic value. Section 2.3 presents the calculation parameters, including the prices, transport distances, and emission factors of raw materials. Monte Carlo simulation is used to consider the uncertainty, and the medians of the calculation results are the representative value. Section 2.4 describes the method of FAGC mixtures collection. Section 2.5 describes the method of FAGC mixture normalization and standardization, which considers the variations of costs and CO_2 emissions with the solid content and moduli of Na_2SiO_3 solutions.

Section 2.6 describes the calculation method of equivalent CC mixtures. Section 2.7 presents an illustrative example.

2.1 CO_2 avoidance cost

The CO_2 avoidance cost of GC is calculated using Eq. (1). An example is used to illustrate the concept of CO_2 avoidance cost. Suppose a GC mixture is 10 USD/m^3 more expensive than CC, but its CO_2 emissions are 100 $kgCO_2/m^3$ lower than CC. It means paying 10 USD to reduce 100 kg of CO_2 emissions. Therefore, the CO_2 avoidance cost C_{CO_2} is 100 USD/tCO_2. As a benchmark, capturing CO_2 from cement plants has been evaluated to have a CO_2 avoidance cost of 55 USD/tCO_2 in China's demonstration project [27]. $C_{CO_2} > 0$ means that additional costs need to pay to reduce carbon emissions. $C_{CO_2} < 0$ means that using this technology can reduce costs while reducing CO_2 emissions.

$$C_{CO_2} = (Cost_{GC} - Cost_{CC})/(E_{CC} - E_{GC}) \times 1000, E_{GC} < E_{CC} \quad (1)$$

where

C_{CO_2} is the CO_2 avoidance cost of GC, USD/tCO_2 (1 USD = 6.9 CNY in 2022);

CC is set as the cement concrete with the same binder volume and compressive strength as GC, which references Habert and Ouellet-Plamondon [32] and Shobeiri et al. [18]; Cement concrete in this study uses 30% SCMs (Supplementary Cementitious Materials) and 70% OPC (ordinary Portland cement) as the binder. Fly ash is used as the SCMs in this study. This blended cement concrete has been widely well-studied, commercialized, and standardized [32-36]. Its cost and CO_2 emissions are much lower than cement concrete produced using 100% OPC, and it is used as the reference concrete in the work of Habert and Ouellet-Plamondon [30]. Some studies use cement concrete produced using 100% OPC as the reference concrete [18,37], which overestimates the carbon emission advantages of geopolymer and underestimates the cost disadvantage of geopolymer.

$Cost_{CC}$ and $Cost_{GC}$ are the costs of CC and GC, USD/m^3.

E_{CC} and E_{GC} are the CO_2 emissions of CC and GC, $kgCO_2/m^3$;

2.2 Costs and CO_2 emissions of CC and FAGC

The calculation method references Van den Heede and De Belie [38], Turner and Collins [37], Yang et al. [39], Salas et al. [40], Habert and Ouellet-Plamondon [32], and Shobeiri et al. [18], as shown

in Eqs. (2-5). The costs and CO_2 emissions of concrete are mainly from the production and transportation of concrete raw materials. Besides, the costs and CO_2 emissions from the energy use of heat curing are considered for FAGC. FAGC usually requires heat curing (e.g., 80℃ for 24 hours) to obtain a desired degree of geopolymerisation and therefore compressive strength.

$$E_{CC} = E_{MatProd} + E_{MatTrans} = \sum_{i=1}^{n} EF_i \times M_i + \sum_{i=1}^{n} EFT_i \times M_i \times D_i \quad (2)$$

$$Cost_{CC} = Cost_{MatProd} + Cost_{MatTrans} = \sum_{i=1}^{n} UP_i \times M_i + \sum_{i=1}^{n} UPT_i \times M_i \times D_i \quad (3)$$

$$E_{FAGC} = E_{MatProd} + E_{MatTrans} + E_{Curing}$$

$$= \sum_{i=1}^{n} EF_i \times M_i + \sum_{i=1}^{n} EFT_i \times M_i \times D_i + EF_{Eng} \times Eng_{Curing} \quad (4)$$

$$Cost_{FAGC} = Cost_{MatProd} + Cost_{MatTrans} + Cost_{Curing}$$

$$= \sum_{i=1}^{n} UP_i \times M_i + \sum_{i=1}^{n} UPT_i \times M_i \times D_i + UP_{Eng} \times Eng_{Curing} \quad (5)$$

where

$E_{MatProd}$, $E_{MatTrans}$, and E_{Curing} are the CO_2 emissions from the raw material production, raw material transportation, and heat-curing, kg/m^3;

$Cost_{MatProd}$, $Cost_{MatTrans}$, and $Cost_{Curing}$ are the costs from the raw material production, raw material transportation, and heat-curing, USD/m^3;

EF_i is the CO_2 emission factor of the *i*th raw material in concrete, kgCO_2/kg;

CC involves coarse and fine aggregates, Portland cement, SCMs (fly ash in this study), admixture (e.g., superplasticizer) and water;

FAGC involves coarse and fine aggregates, fly ash, NaOH, Na_2SiO_3 and water; The water-reducing admixture is not involved because the geopolymer system lacks effective water-reducing admixture [6];

M_i is the mass dosage of the *i*th raw material in concrete, kg/m^3;

EFT_i is the CO_2 emission factor of transportation of the *i*th raw material, kgCO_2/(kg·km);

D_i is the transportation distance of the *i*th raw material, km;

UP_i is the unit price of the *i*th raw material in concrete, USD/kg;

UPT_i is the unit price of transportation of the *i*th raw material, USD/(kg·km);

EF_{Eng} is the CO_2 emission factor of the energy used (e.g., electricity), kgCO_2/kWh;

Eng_{Curing} is the energy use of heat-curing, kWh;

UP_{Eng} is the unit price of the energy used (e.g., electricity), USD/kWh.

A key issue is estimating the energy use of curing Eng_{Curing} at different curing temperatures and times. Salas et al. [40] and Shobeiri et al. [18] stated that the energy is required to heat the concrete to the curing temperature and to compensate for the heat loss, so Eq. (6) is developed to estimate Eng_{Curing}. The ambient temperature is assumed as 25℃.

$$Eng_{Curing} = Eng_{Heat} + Eng_{Loss} = M \times c \times (T - 25℃) + P \times t, T > 25℃ \quad (6)$$

where

Eng_{Heat} is the energy required to heat the concrete to the curing temperature;

Eng_{Loss} is the energy required to compensate for the heat loss;

M is the mass of FAGC, kg;

c is the specific heat capacity of FAGC which is assumed to be 700 (J/kg℃) according to Shobeiri et al. [18];

T is the curing temperature, ℃;

P is the heating power to compensate for heat loss and keep the temperature constant, kW;

t is the heat-curing time, hour (h).

Based on the heat transfer theory, P is proportional to the difference between the curing temperature T and the ambient temperature of 25℃ [40]. P at $T = 25℃$ is 0. P at $T = 80℃$ is assumed to be 600 W for 1 m^3 concrete according to Shobeiri et al. [18]. Therefore, Eq. (7) is developed to calculate P at different T. This assumption can approximate the real situation. Nisbet et al. [41] give an actual curing energy of 62 MJ/m^3 for concrete curing at 54 °C for 24 h, while the curing energy is estimated as 76.85 MJ/m^3 using Eqs. (6) and (7), close to 62 MJ/m^3.

$$P = (T - 25℃)/(80℃ - 25℃) \times 600W \quad (7)$$

Another key issue is determining the CO_2 emission factor of fly ash EF_{FlyAsh}. The current consensus is that fly ash is considered an industrial by-product of coal electricity rather than a waste, so the CO_2 emissions from coal electricity should be allocated to fly ash based on the economic value, as shown in Eq. (8) [42]. Therefore, Eq. (9) is developed to calculate EF_{FlyAsh}.

$$\frac{E_{FlyAsh}}{E_{CoalElectricity}} = \frac{m_{FlyAsh} \times UP_{FlyAsh}}{m_{FlyAsh} \times UP_{FlyAsh} + 1kWh \times UP_{Electricity}} \quad (8)$$

$$EF_{FlyAsh} = \frac{E_{FlyAsh}}{m_{FlyAsh}} = \frac{EF_{CoalElectricity} \times UP_{FlyAsh}}{m_{FlyAsh} \times UP_{FlyAsh} + 1kWh \times UP_{Electricity}} \quad (9)$$

where

m_{FlyAsh} is the mass of fly ash produced during 1 kWh of coal electricity, 0.125kg; In 2019, China's coal electricity generation was 5.22×10^{12} kWh [43], and the fly ash production was 6.55×10^{11} kg [29], which means that about 0.125 kg of fly ash is produced during 1 kWh of coal electricity;

$EF_{CoalElectricity}$ is the CO_2 emission factor of coal electricity, 0.838 kgCO_2/kWh [43];

UP_{FlyAsh} is the unit price of fly ash, USD/kg;

$UP_{Electricity}$ is the unit price of electricity, USD/kWh.

2.3 Calculation parameters and Monte Carlo simulation

The calculation parameters are listed in Table 1. Considering the uncertainty of the prices, transport distances, and emission factors of raw materials, we do not calculate a definite CO_2 avoidance cost, but rather calculate the probability distribution of the CO_2 avoidance cost using Monte Carlo simulation. Monte Carlo simulation is a common method for the uncertainty analysis of life cycle assessment [44,45]. As shown in Fig. 1, the Monte Carlo simulation in this study involves the following steps:

1) determining the variation ranges of uncertain parameters, such as raw material prices and transport distances, and assuming these parameters follow the uniform distribution, i.e., equal probability that they will take on any number within their respective ranges;

2) randomly sampling once from the probability distribution of each parameter;

3) calculating the CO_2 avoidance cost based on the obtained random samples;

4) repeating steps 2 and 3 50000 times to obtain 50000 samples of the CO_2 avoidance cost, and then obtain the frequency distribution of the CO_2 avoidance cost, which approximates the probability distribution. The median CO_2 avoidance cost $C_{CO_2,50\%}$ is the representative value of the CO_2 avoidance cost used for the analysis. $C_{CO_2,50\%}$ lower than a specific value means a more than 50% probability of the CO_2 avoidance cost being lower than the specific value. $C_{CO_2,50\%} < 55\ USD/tCO_2$ means there is a more than 50% probability that C_{CO_2} is lower than 55 USD/tCO_2.

208 **Table 1 Calculation parameters**

Parameters	Values	Sources
Raw materials details		
Type of cement	P·O 42.5	
Type of Na_2SiO_3 solution	8.55% of Na_2O and 26.87% of SiO_2	
Unit prices		
NaOH	350~450 USD/t	[46]
Na_2SiO_3 solution	144.93~217.39 USD/t (1000~1500 CNY/t)	
Fly ash	1.449~4.348 USD/t (10~30 CNY/t)	[47]
Cement	66.667~72.464 USD/t (460~500 CNY/t)	[48]
Aggregate	8.696 USD/t (60 CNY/t)	[48]
Admixture	815.94 USD/t (5630 CNY/t)	[49]
Water	0.435 USD/t (3 CNY/t)	
Emission factors ($kgCO_2/kg$)		
NaOH	1.04~1.59	[50]
Na_2SiO_3 solution	0.3755	[32]
Fly ash	varies with the price	[42]
Cement	0.732	[51]
Aggregate	0.00398	[51]
Admixture	0.72	[51]
Water	0.000148	[51]
Transport distance (km)		
NaOH	50~300	[52]
Na_2SiO_3 solution	50~300	[52]
Fly ash	50~300	[52]
Cement	50~300	[52]
Aggregate	50	
Admixture	50~300	[52]
Water	0	
Transportation details		
Transportation mode	Road	
Unit price	0.0696 USD/(t·km) (0.48 CNY/(t·km))	[53]
Emission factors ($kgCO_2/(kg·km)$)	$1.37·10^{-4}$	[51]
Curing details		
Energy	Electricity	
Unit price	0.08087 USD/kWh (0.55 CNY/kWh)	[24]
Emission factor ($kgCO_2/kWh$)	0.55	[24]

209

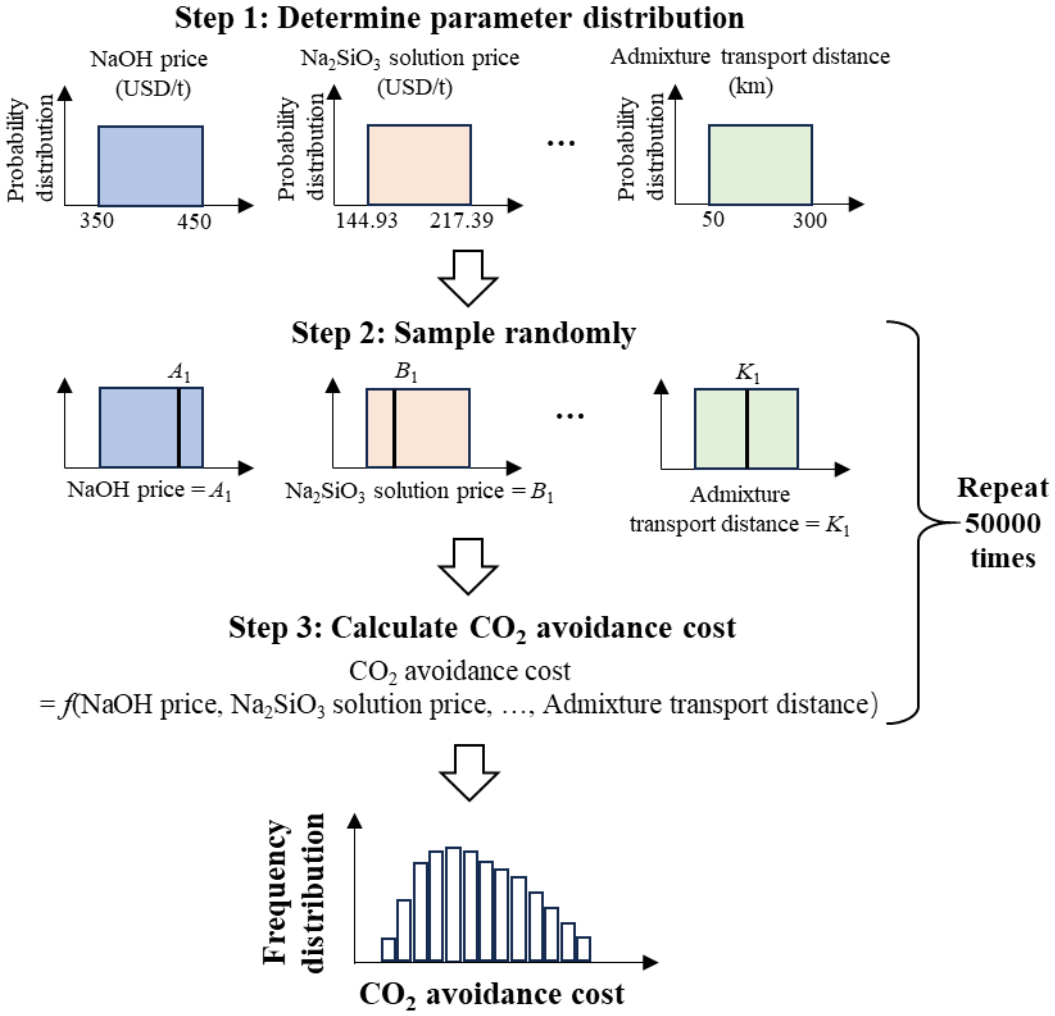

Fig. 1 Monte Carlo simulation

Notes:

1) The prices presented in Chinese Yuan (CNY) are converted into US Dollar (USD) at the 2022 rate (1 USD = 6.9 CNY).

2) P·O 42.5 cement, classified using the Chinese standard GB 175-2007 [54] and almost equal to CEM II/A 42.5N cement in the European standard EN 197-1 [55], is considered in this study. P·O means ordinary Portland cement that contains 80%-95% of clinker and 5%-20% of other materials such as slag or fly ash by mass; The number 42.5 means the strength class.

3) Different Na_2SiO_3 solutions with different solid content and moduli are used in the literature. L-330-37 Na_2SiO_3 solution with Na_2O content ≥8.2% and SiO_2 content ≥26%, classified using the Chinese standard GB/T 4209-2022 [56], is common in the China market, so it is considered the

223 standard Na_2SiO_3 solution in this study. Based on our survey of four Na_2SiO_3 solutions in the market,
224 the average Na_2O and SiO_2 content are 8.55% and 26.87%. The costs and CO_2 emissions of other
225 types of Na_2SiO_3 solutions can be obtained by adding or deducting NaOH or water in the standard
226 Na_2SiO_3 solution. Please refer to Section 2.5 for the conversion details.
227 4) Based on our survey, only in Northwest China can the fly ash price be as low as 1.449~4.348
228 USD/t (10~30 CNY/t) due to the high production and low utilization of fly ash. In Southeastern
229 China, the fly ash price exceeds 21.7 USD/t (150 CNY/t), and almost all fly ash is used to produce
230 cement and concrete.
231 5) The CO_2 emission factor of NaOH varies with the electricity sources and production technologies
232 [50].
233 6) The transportation distances of NaOH, Na_2SiO_3 solution, fly ash, cement and admixture are set
234 at 50~300 km considering these raw materials are locally available [52]. The transportation distance
235 of aggregate is fixed at 50 km. Setting the aggregate transportation distance to any distance does not
236 affect the final result because the aggregate content in FAGC and CC is set to be equal in the
237 calculation.
238 7) The CO_2 emission factor of coal electricity in China is 0.838 $kgCO_2/kWh$, which is used to
239 calculate the CO_2 emission factor of fly ash, while 0.55 $kgCO_2/kWh$ is the average CO_2 emission
240 factor of electricity covering coal electricity, hydropower, etc. It is used to calculate the CO_2
241 emission from electricity use.
242
243 **2.4 FAGC mixtures collection**
244 A total of 486 FAGC mixtures from 75 previously published studies are collected [57-131]. The
245 details of each mixture include the mass of each component, heat-curing temperature, heat-curing
246 time, total curing time, mass fraction and density of NaOH solution, Na_2O content, SiO_2 content
247 and density of Na_2SiO_3 solution, compressive strength and tested specimen type. They all meet the
248 following criteria:
249 1) Only fly ash is used as a precursor, only NaOH and Na_2SiO_3 are used alone or in combination as
250 activators, and only natural aggregates are used.
251 2) The mass of each component, heat-curing temperature, heat-curing time and total curing time are
252 reported completely.

3) The mass fraction or molar concentration of NaOH solution and the solid content and modulus of Na_2SiO_3 solution are reported.

4) The 28th-day compressive strength or the early compressive strength after heat-curing and the type of specimen for the compressive strength test are reported.

5) Their compressive strength is at least 20 MPa. Mixtures with compressive strength of lower than 20 MPa are excluded as their application in civil engineering is limited.

2.5 FAGC mixture normalization and standardization

2.5.1 FAGC mixture normalization

The collected FAGC mixtures require normalization to 1 m^3. First, for each mixture, the original volume $V_{original}$ is calculated based on the mass of each component and the air content of 3%, as shown in Eq. (10).

$$V_{original} = \left(\sum_{i=1}^{n} M_{i,original}/\rho_i\right)/(1 - Air\ content) \quad (10)$$

where

$M_{i,original}$ is the mass of the *i*th raw material, kg;

ρ_i is the density of the *i*th raw material, kg/m^3; The density of aggregate, fly ash and water are assumed to be 2600 kg/m^3, 2000 kg/m^3 and 1000 kg/m^3; The density of NaOH solution and Na_2SiO_3 solution are determined by the solid content;

$Air\ content$ is assumed to be 3% for FAGC according to Provis et al. [132].

Then, the normalized mass of the *i*th raw material $M_{i,normalized}$ is calculated as shown in Eq. (11).

$$M_{i,normalized} = M_{i,original}/V_{original} \times 1m^3 \quad (11)$$

2.5.2 Equivalent alkali-activated solution using standard Na_2SiO_3 solution

Na_2SiO_3 solutions with various solid content and moduli are used in the literature. The costs and CO_2 emissions of these Na_2SiO_3 solutions also vary. A standard Na_2SiO_3 solution with a Na_2O content of 8.55% and SiO_2 content of 26.87% is considered in this study. We can use the standard Na_2SiO_3 solution to obtain an equivalent alkali-activated solution with the same Na_2O, SiO_2 and H_2O content as the alkali-activated solution used in the literature by adding or deducting NaOH and

water. The equivalent alkali-activated solution is used to calculate the cost and CO_2 emissions from materials production.

For each mixture, the Na_2O, SiO_2 and H_2O content in the alkali-activated solution can be obtained by Eqs. (12-14).

$$M_{\mathrm{Na_2O}} = M_{\mathrm{NaOH}solution} \times \mathrm{NaOH\%} \times 62/80 + M_{\mathrm{Na_2SiO_3}solution} \times \mathrm{Na_2O\%} \quad (12)$$

$$M_{\mathrm{SiO_2}} = M_{\mathrm{Na_2SiO_3}solution} \times \mathrm{SiO_2\%} \quad (13)$$

$$M_{\mathrm{H_2O}} = M_{\mathrm{NaOH}solution} + M_{\mathrm{Na_2SiO_3}solution} + M_{ExtraWater} - M_{\mathrm{Na_2O}} - M_{\mathrm{SiO_2}} \quad (14)$$

where

$M_{\mathrm{Na_2O}}$, $M_{\mathrm{SiO_2}}$, $M_{\mathrm{H_2O}}$ are the Na_2O, SiO_2 and H_2O content in the alkali-activated solution;

$M_{\mathrm{NaOH}solution}$ is the mass of NaOH solution;

$\mathrm{NaOH\%}$ is the NaOH content of NaOH solution (e.g., the NaOH content is 39.34% for 14 mol/L NaOH solution);

$M_{Na_2SiO_3solution}$ is the mass of Na_2SiO_3 solution;

$\mathrm{Na_2O\%}$ and $\mathrm{SiO_2\%}$ are the Na_2O and SiO_2 content in Na_2SiO_3 solution;

$M_{ExtraWater}$ is the mass of extra water that some studies add in the alkali-activated solution besides NaOH and Na_2SiO_3 solutions.

Then, the equivalent alkali-activated solution using standard Na_2SiO_3 solution can be obtained by Eqs. (15-17).

$$M_{E-\mathrm{Na_2SiO_3}solution} = M_{\mathrm{SiO_2}}/0.2687 \quad (15)$$

$$M_{E-\mathrm{NaOH}solid} = \left(M_{\mathrm{Na_2O}} - 0.0855 \times M_{E-\mathrm{Na_2SiO_3}solution}\right)/62 \times 80 \quad (16)$$

$$M_{E-water} = M_{\mathrm{NaOH}solution} + M_{\mathrm{Na_2SiO_3}solution} - M_{E-\mathrm{Na_2SiO_3}solution} - M_{E-\mathrm{NaOH}solid} \quad (17)$$

where $M_{E-\mathrm{Na_2SiO_3}solution}$, $M_{E-\mathrm{NaOH}solid}$, and $M_{E-water}$ are the standard Na_2SiO_3 solution, NaOH solid and extra water content in the equivalent alkali-activated solution.

2.5.3 Equivalent compressive strength of standard specimen

Different specimen types are used for the compressive strength test in the literature. For the same mixture, compressive strength results vary with the specimen types. The 150 mm cubes are considered the standard specimens in this study. The compressive strength of other specimens is converted to the equivalent compressive strength of the standard specimen. The conversion factors are shown in Table 2 [18,123,133]. For example, for C60 concrete, according to Table 2, we can multiply the 100×200mm cylinder compressive strength by the specific conversion factor 1.129 to obtain the 150 mm cube compressive strength. Some literature uses 76×152mm cylinders whose compressive strength is considered equal to that of 100×200mm cylinders [134,135].

Table 2 Conversion factors of compressive strength

Strength (MPa)	100mm cube	100×200mm cylinder	150×300mm cylinder
20~50		1.214	1.25
50~60		1.17	1.205
60~70	0.95	1.129	1.163
70~80		1.11	1.143
>80		1.091	1.124

2.6 Equivalent CC mixture

To provide a meaningful comparison between FAGC and CC, they should have the same compressive strength and binder paste volume [18,32]. We can use FAGC's compressive strength and paste volume and CC's strength equation based on the water to binder ratio (w/b) to calculate the equivalent CC mixture.

First, Eq. (18), an empirical equation proposed by Chinese standard JGJ 55-2011 "Specification for mix proportion design of ordinary concrete" is used to calculate w/b in the equivalent CC mixture [33].

$$w/b = 0.53 \times f_b/(f_c + 0.106 \times f_b) \quad (18)$$

where f_b is the binder strength which is assumed to be 36.975 MPa according to JGJ 55-2011 when

replacing 30% P.O 42.5 cement with fly ash; f_c is the target 28-day compressive strength.

Eq. (18) is derived from the classical Bolomy equation, as shown in Eq. (19). The key parameters are obtained through data fitting by Chinese standard JGJ 55-2011. We validate the equation and assumptions for key parameters using the data collected from the literature [136-141], as shown in Fig. 2.

$$Bolomy\ equation: f_c = K\left(\frac{1}{w/b} - a\right) \rightarrow\ w/b = K/(f_c + Ka) \tag{19}$$

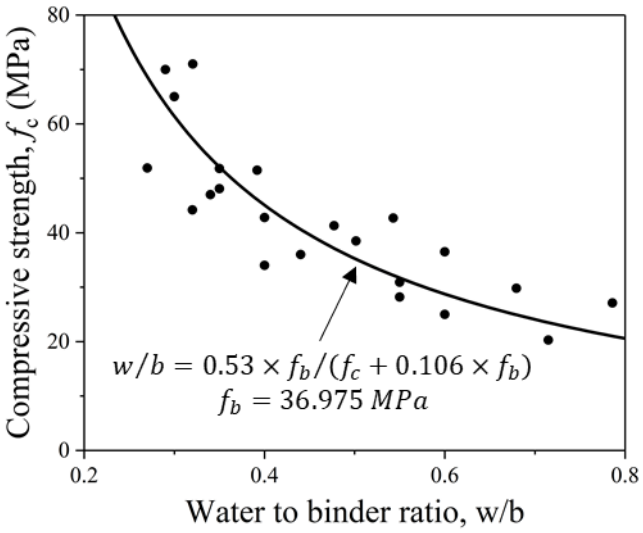

Fig. 2 Validation of mix design equation of CC

Then, the cement dosage $M_{Cement-CC}$, fly ash dosage $M_{FlyAsh-CC}$ and water dosage $M_{Water-CC}$ in CC are determined by solving Eqs. (20-22).

$$\frac{M_{Cement-CC}}{\rho_{Cement}} + \frac{M_{FlyAsh-CC}}{\rho_{FlyAsh}} + \frac{M_{Water-CC}}{\rho_{Water}} + Air\ content = V_{paste} \tag{20}$$

$$M_{FlyAsh-CC}/\left(M_{Cement-CC} + M_{FlyAsh-CC}\right) = 0.3 \tag{21}$$

$$M_{Water-CC}/\left(M_{Cement-CC} + M_{FlyAsh-CC}\right) = w/b \tag{22}$$

where $\rho_{Cement}, \rho_{Flyash}, \rho_{Water}$ are the density of cement, fly ash and water which are assumed to be 3000 kg/m^3, 2000 kg/m^3 and 1000 kg/m^3;

$Air\ content$ is assumed to be 1% for CC;

V_{paste}, calculated by Eq. (23), is the paste volume of FAGC and CC.

$$V_{paste} = \frac{M_{FlyAsh}}{\rho_{FlyAsh}} + \frac{M_{NaOHsolution}}{\rho_{NaOHsolution}} + \frac{M_{Na_2SiO_3solution}}{\rho_{Na_2SiO_3solution}} + \frac{M_{ExtraWater}}{\rho_{Water}} + 3\% \quad (23)$$

Finally, if $M_{Water-CC}$ is less than 200 kg/m^3, the superplasticizer needs to be added at 1% of the binder content ($M_{Cement-CC} + M_{FlyAsh-CC}$).

2.7 Illustrative example: Mixture 1

Fig. 3 shows the distribution of CO_2 emissions and costs of Mixture 1 and the equivalent CC mixture in 50000 Monte Carlo runs. The representative values are the medians $E_{FAGC,50\%}$, $E_{CC,50\%}$, $Cost_{FAGC,50\%}$, and $Cost_{CC,50\%}$, which are 139.55 kgCO_2/m^3, 279.52 kgCO_2/m^3, 61.31 USD/m^3, and 53.9 USD/m^3.

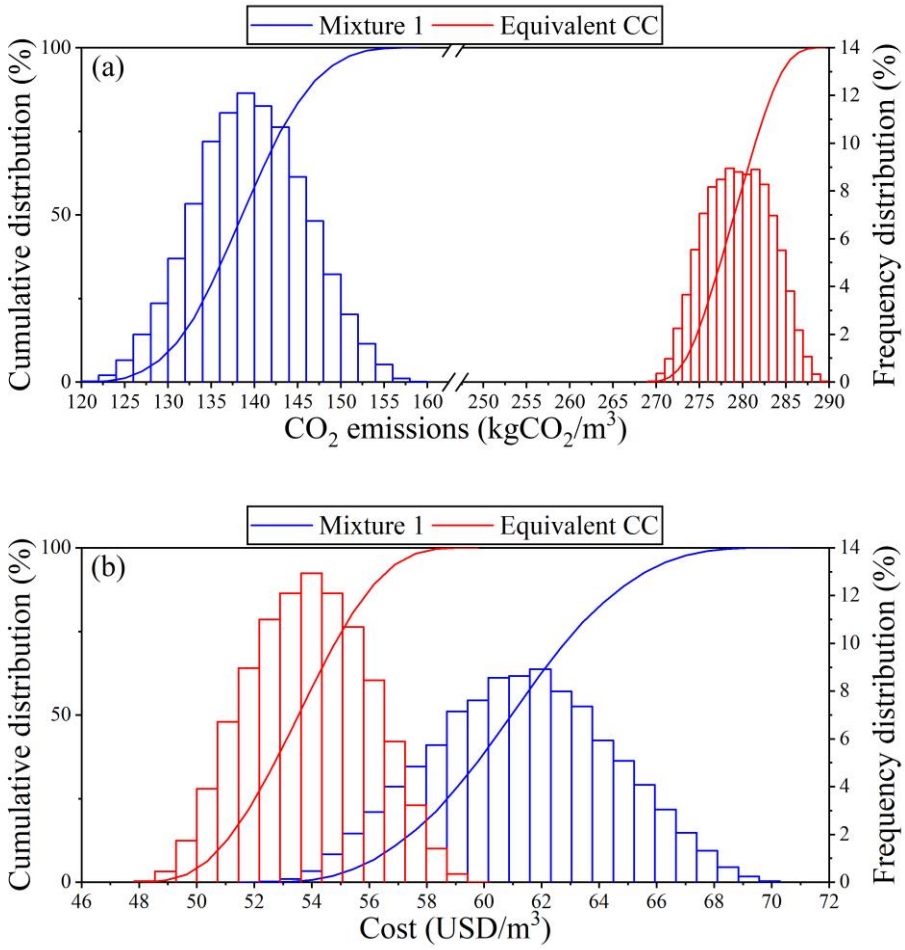

Fig. 3 Distribution of CO_2 emissions and costs of Mixture 1 and the equivalent CC mixture in 50000 Monte Carlo runs

The CO_2 emissions reduction R_{CO_2} of FAGC is calculated using Eq. (24). Fig. 4 shows the distribution of CO_2 emissions reduction of Mixture 1 in 50000 Monte Carlo runs. Compared to equivalent CC, Mixture 1 can reduce carbon emissions by at least 43.15%. $R_{CO_2,50\%}$ is 50.06%.

$$R_{CO_2} = (E_{CC} - E_{FAGC})/E_{CC} \quad (24)$$

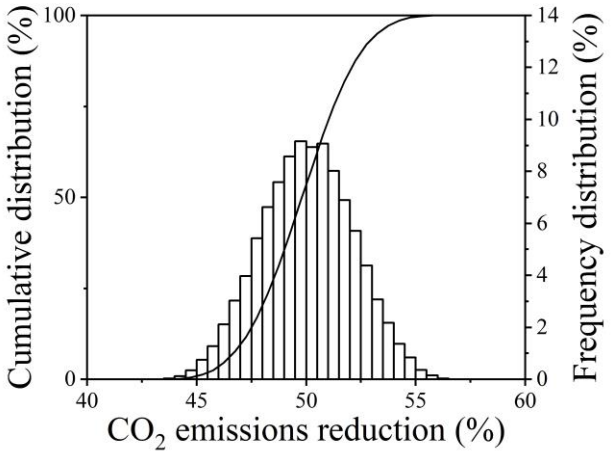

Fig. 4 Distribution of CO_2 emissions reduction of Mixture 1 in 50000 Monte Carlo runs

Fig. 5 shows the distribution of CO_2 avoidance cost C_{CO_2} of Mixture 1 in 50000 Monte Carlo runs. There is only a small probability of $C_{CO_2} < 0$. $C_{CO_2,50\%}$ is 52.91 USD/tCO_2, which is lower than the cost of capturing CO_2 from cement plants (55 USD/tCO_2).

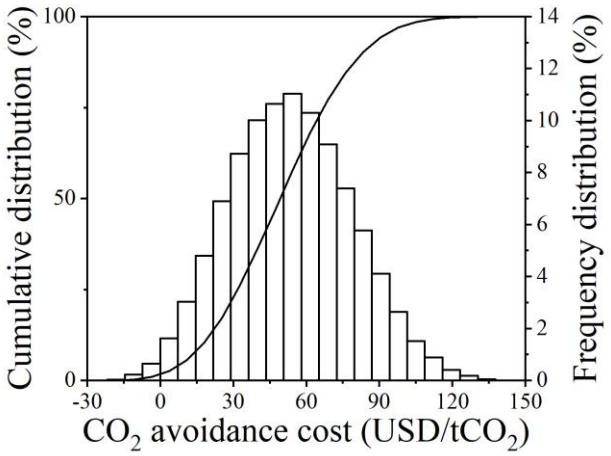

Fig. 5 Distribution of CO_2 avoidance cost of Mixture 1 in 50000 Monte Carlo runs

$E_{FAGC,50\%}$, $E_{CC,50\%}$, $Cost_{FAGC,50\%}$, $Cost_{CC,50\%}$, $R_{CO_2,50\%}$, and $C_{CO_2,50\%}$ of the 486 mixtures are used as the representative values in the following analysis.

3. Results and discussion

3.1 Costs and CO_2 emissions of FAGC and equivalent CC

Fig. 6 compares the costs and CO_2 emissions of FAGC and equivalent CC. The results are presented as a function of compressive strength. Similar results on CO_2 emissions have been shown by Shobeiri et al. [18], so the costs are the focus of this work. Although FAGC is lower in CO_2 emissions than CC in most cases, FAGC is more expensive than CC. We noticed that in some cases, the cost of FAGC can be close to or even lower than CC. Identifying the features of low-cost FAGC is worth studying.

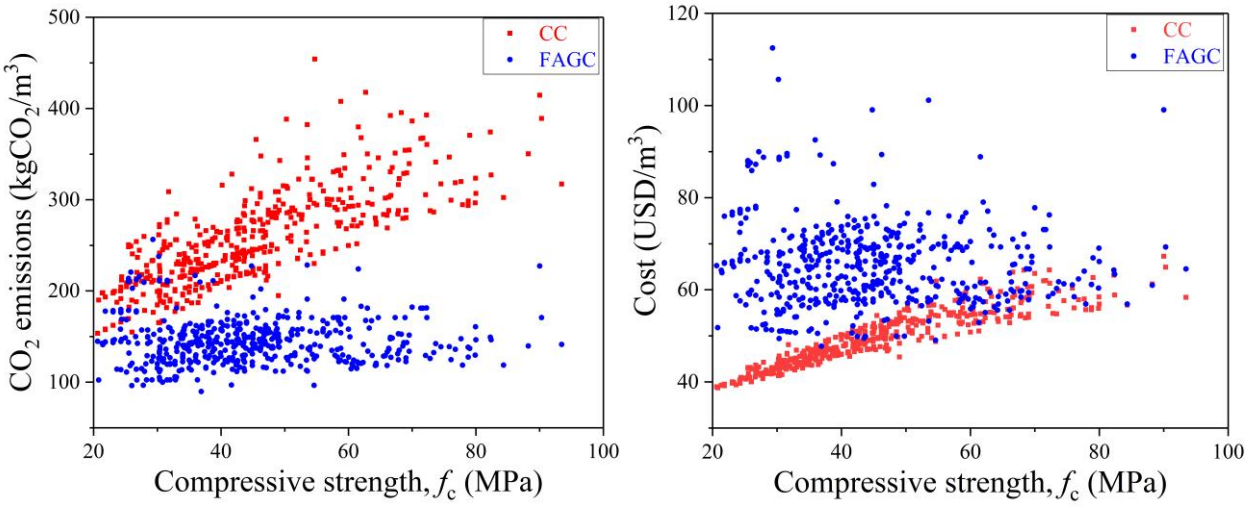

(a) **(b)**

Fig. 6 Costs and CO_2 emissions of FAGC and equivalent CC (Each data point is the median of the Monte Carlo results)

The cost and CO_2 emissions of CC increase with the compressive strength. However, the relationship is not observed in FAGC. For CC, the cost and CO_2 emissions mainly depend on the cement dosage, and the high strength needs a high cement dosage, so the high strength is associated with the high cost and CO_2 emissions [142]. For FAGC, the cost and CO_2 emissions mainly depend on the activator (Na_2O and SiO_2 in the alkali-activated solution) dosage, as shown in Fig. 7. However,

a high activator dosage is not associated with high strength. For a given fly ash, a high activator dosage usually leads to high strength [123,143]. However, fly ash is only a by-product rather than a well-designed industrial product like cement. The fly ash from different sources varies considerably in physicochemical characteristics [144-146]. To achieve sufficient strength, some fly ash only requires a small amount of alkali activator, while others require a large amount of alkali activator. Fly ash suitable for alkali activation is often considered to have the following characteristics: high amorphous content, suitable amorphous Si/Al ratio, and high specific surface area [144-146]. A direct and easy method to evaluate fly ash is trial, i.e., creating some experimental groups by varying the activator dosage and then testing the compressive strength [123].

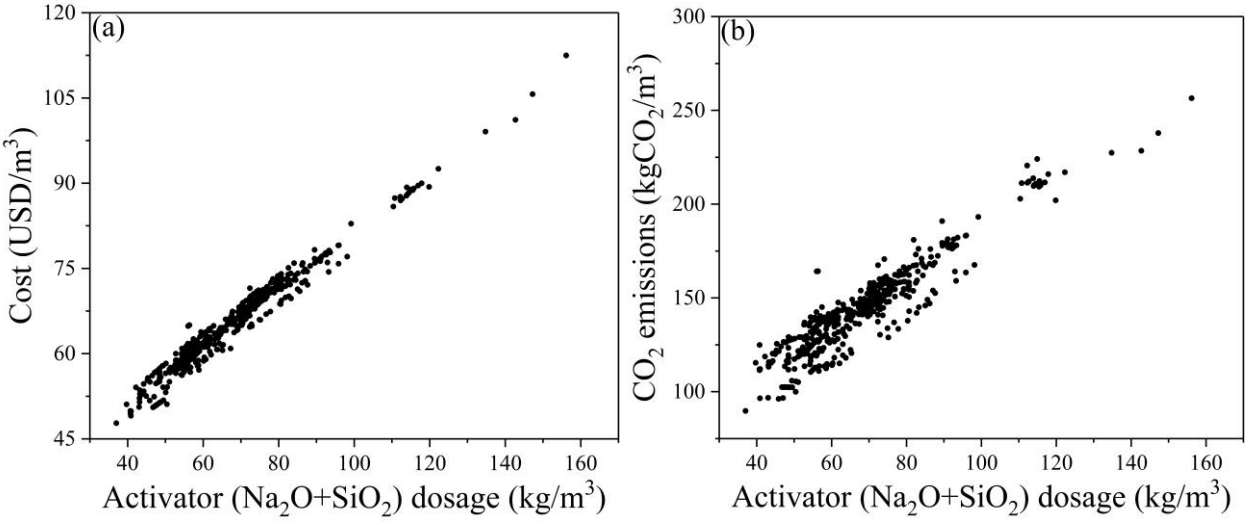

Fig. 7 Relationships between costs and CO_2 emissions of FAGC and activator dosage

3.2 CO_2 avoidance cost of FAGC and activator index

Two benchmarks to evaluate the cost of FAGC are CC and capturing CO_2 from cement plants, respectively. FAGC with a lower cost than CC is recommended use, but it is still acceptable that the cost of FAGC is higher than CC but lower than capturing CO_2 from cement plants. $C_{CO_2,50\%} < 0$ means a more than 50% probability of the cost of FAGC being lower than CC. $C_{CO_2,50\%} < 55$ USD/tCO_2 means a more than 50% probability of the cost of FAGC being lower than capturing CO_2 from cement plants. Only 107 of 486 FAGC mixtures are more economical than capturing CO_2 from cement plants, 7 of which have negative CO_2 avoidance costs.

The cost and CO_2 emissions of CC increase with the compressive strength. However, those of FAGC are independent of compressive strength. They increase with the activator dosage. Therefore, the low CO_2 avoidance cost C_{CO_2} of FAGC, a result of low cost and CO_2 emissions of FAGC and high cost and CO_2 emissions of equivalent CC, is associated with low activator dosage and high compressive strength. To quantify the relationship, this study proposes the activator index (*Ai*), the activator dosage ($kg \cdot m^{-3}$) necessary to deliver 1 MPa of compressive strength. The $C_{CO_2,50\%}$ decreases with the decrease in *Ai*, as shown in Fig. 8a.

The cost index (*Ci*), calculated using Eq. (25), is proposed to better present the relationship between C_{CO_2} and *Ai*. The number 100 is introduced to compensate for the negative value of C_{CO_2} so that logarithmic operations can be performed. $Ci < 0$ equals to $C_{CO_2,50\%} < 0$. $Ci < 1$ equals to $C_{CO_2,50\%} < 55$ USD/tCO_2. Fig. 8b shows the linear relationship between *Ci* and *Ai*, but R^2<0.9 shows the correlation is not strong enough.

$$Ci = log_{1.55}\left(\left(C_{CO_2} + 100\right)/100\right) \quad (25)$$

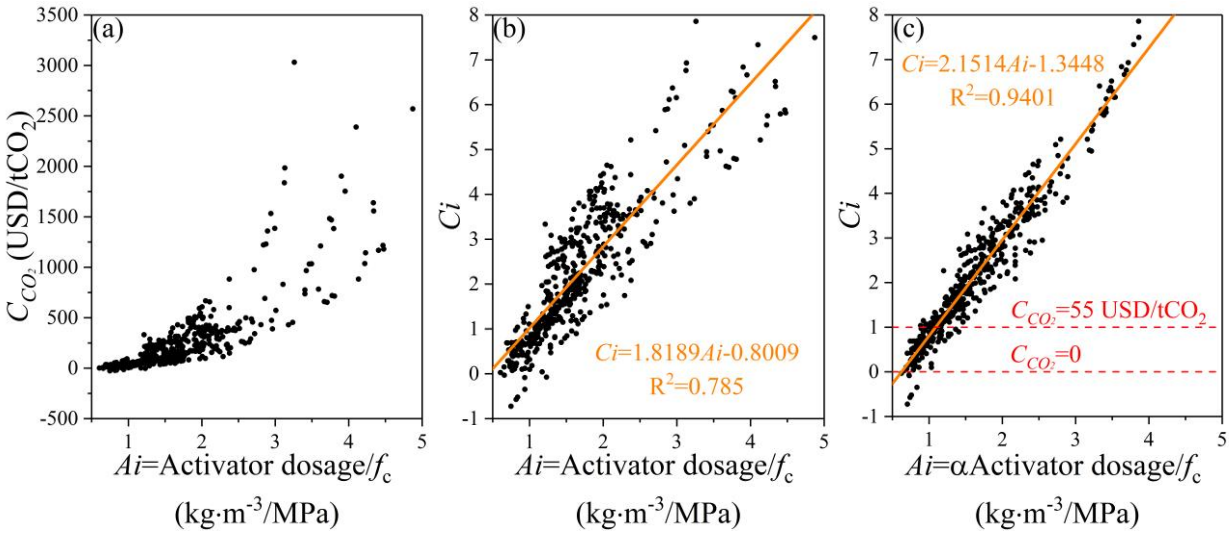

Fig. 8 Relationship between CO_2 avoidance cost of FAGC and activator index (*Ai*)

A corrected activator index *Ai*, calculated using Eq. (26), is proposed. We noticed that the paste volume also affects the CO_2 avoidance cost C_{CO_2} besides the activator dosage and compressive strength. The high paste volume for FAGC means more fly ash, while for CC, it means more cement. Cement is much more cost- and emission-intensive than fly ash, so FAGC with a higher paste

446 volume is easier to acquire a low C_{CO_2}. Meanwhile, a concrete mixture with a paste volume of 35%
447 is recommended, which is well considered to perform well in workability, strength and durability
448 [147,148]. Therefore, the effect of paste volume is eliminated through introducing a dimensionless
449 volume correction factor $\alpha = \frac{0.35\ m^3}{V_{paste}}$.

450 $$Ai = \alpha\, Activator\ dosage/f_c \quad (26)$$

451

452 Fig. 8c shows the strong linear correlation between *Ci* and *Ai*. According to the fitted linear equation,
453 $Ai < 1.09$ kg·m^{-3}/MPa and $Ai < 0.625$ kg·m^{-3}/MPa correspond to the CO_2 avoidance cost of FAGC
454 lower than 55 USD/tCO_2 and 0. The *Ai* value can be used to evaluate the economic feasibility of a
455 FAGC mixture. The CO_2 avoidance cost decreases as the *Ai* value decreases. The critical *Ai* value
456 is 1.09 kg·m^{-3}/MPa. This *Ai*-based criterion can be extended to geopolymer concrete using other
457 precursors, as NaOH and Na_2SiO_3 are mainly used as activators. However, it can be foreseen that
458 the critical *Ai* value for geopolymer concrete using other precursors is smaller than 1.09, as the
459 precursor used in this study, fly ash in northwest China, is much cheaper than other precursors.

460

461 $Ai < 1.09$ kg·m^{-3}/MPa and $Ai < 0.625$ kg·m^{-3}/MPa also correspond to 51.83% and 59.85% emission
462 reductions of FAGC compared with blended cement concrete, as shown in Fig. 9. Note that blended
463 cement concrete has achieved a 20% emission reduction compared to concrete using 100% OPC
464 [32].

465

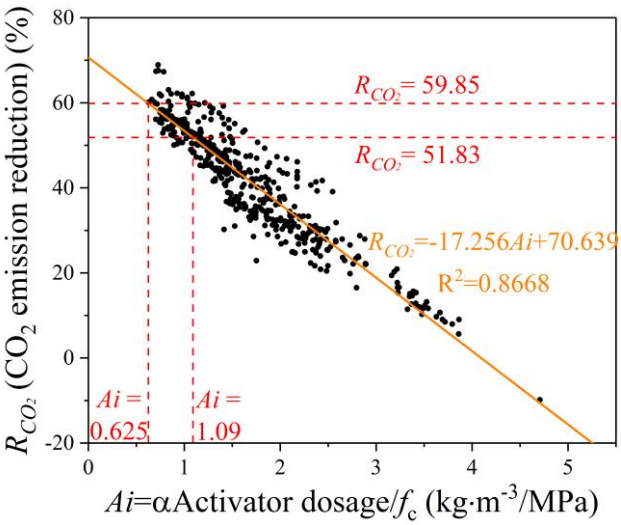

466

467 **Fig. 9 Relationship between CO_2 emission reduction of FAGC and activator index (*Ai*)**

3.3 Relationship between activator dosage and compressive strength

In our previous study [123], we proposed a mix design equation of FAGC, Eq. (27), which describes the relationship between activator dosage and compressive strength and is in accordance with the data in many studies [123,127,128,143,149-151], as shown in Fig. 10. In many studies, the activator dosage is characterized by Na_2O dosage (the mass ratio of Na_2O in the alkali-activated solution to fly ash) and activator modulus (the mass ratio of SiO_2 to Na_2O in the alkali-activated solution). As shown in Fig. 10, the compressive strength of FAGC increases with the Na_2O dosage but then decreases when the Na_2O dosage exceeds a threshold β (around 15%) [149-157]. Note that fly ash is only a by-product rather than a well-designed industrial product like cement. The fly ash from different sources varies considerably in physicochemical characteristics. Therefore, β varies with each fly ash. Similarly, the compressive strength of FAGC increases with the activator modulus but then decreases beyond a threshold α (around 1.0) [149-156]. And α varies with each fly ash. Overall, within the appropriate range (Na_2O dosage $\leq \beta$ and activator modulus $\leq \alpha$), the strength increases with the activator (Na_2O+SiO_2) dosage. Also, the strength decreases with the water content. Drawing on the concept of water/cement ratio in CC, we proposed Eq. (27) [123]. Note that the coefficients a and b also vary with each fly ash and curing condition.

$$f_c = -a\frac{M_{H_2O}}{M_{Na_2O}+M_{SiO_2}} + b \quad (27)$$

Pre-experiments before mix design, creating some experimental groups by varying the Na_2O dosage, activator modulus, and water content, and then testing the respective compressive strength, can indicate the upper limit of Na_2O dosage and activator modulus β and α, and the coefficients a and b in Eq. (27). After determining the water content for target workability, the activator (Na_2O+SiO_2) dosage can be determined by Eq. (27). Then, according to the upper limit of the activator modulus, the Na_2O dosage and SiO_2 dosage can be determined. Finally, according to the upper limit of Na_2O dosage, fly ash dosage can be determined.

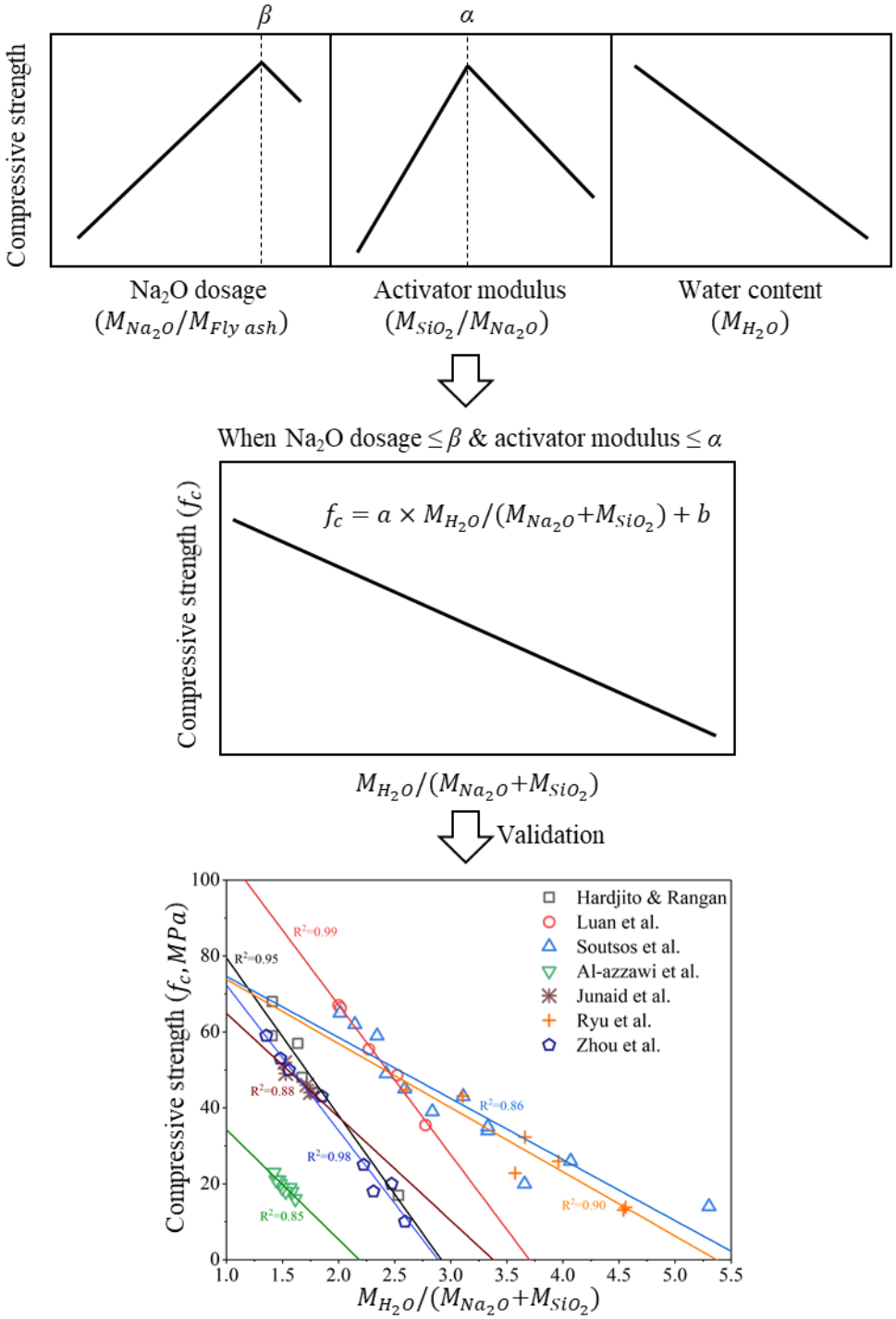

Fig. 10 Relationship between activator dosage and compressive strength (the data from Hardjito & Rangan [128], Luan et al. [123], Soutsos et al. [149], Al-Azzawi et al. [127], Junaid et al. [143], Ryu et al. [150], Zhou et al. [151])

3.4 Application of activator index to aid mix design

Only GC mixtures with lower CO_2 avoidance costs will be considered for use by the industry. This

paper provides a standard for the swift identification of such GC mixtures. Based on the activator index (Ai), geopolymer mixtures can be classified into two categories: the economically acceptable (Ai<1.09), having a lower CO_2 avoidance cost than capturing CO_2 from cement plants, and the economically unacceptable (Ai≥1.09) with a higher CO_2 avoidance cost.

This approach can assist in mix design for achieving the desired strength with high emissions reduction and low cost. Illustratively, two types of fly ash, denoted as Fly ash A (from Luan et al. [123]) and Fly ash B (from Junaid et al. [143]), are considered. Eqs. (28) and (29) represent mix design equations for Fly ash A and Fly ash B, respectively. Upon fixing the water content at 110 kg/m^3 to achieve the target slump, Eqs. (28) and (29) transform into Eqs. (30) and (31). And Eqs. (30) and (31) are plotted in Fig. 11. The line of Ai=1.09 divides Fig. 11 into two regions: economically acceptable (blue region) and economically unacceptable (red region). Only GC mixtures using Fly ash A with strengths exceeding 36 MPa fall within the blue region, signifying lower CO_2 avoidance costs and, consequently, a recommendation for use. Conversely, all GC mixtures using Fly ash B have Ai values higher than 1.09, indicating higher CO_2 avoidance costs than capturing CO_2 from cement plants. Thus, their usage is not recommended, despite achieving adequate strength.

$$Fly\ ash\ A: f_c = -39.422 \times \frac{M_{H_2O}}{M_{Na_2O}+M_{SiO_2}} + 145.93 \quad (28)$$

$$Fly\ ash\ B: f_c = -27.277 \times \frac{M_{H_2O}}{M_{Na_2O}+M_{SiO_2}} + 92.168 \quad (29)$$

$$Fly\ ash\ A: f_c = -39.422 \times \frac{110}{M_{Na_2O}+M_{SiO_2}} + 145.93 \quad (30)$$

$$Fly\ ash\ B: f_c = -27.277 \times \frac{110}{M_{Na_2O}+M_{SiO_2}} + 92.168 \quad (31)$$

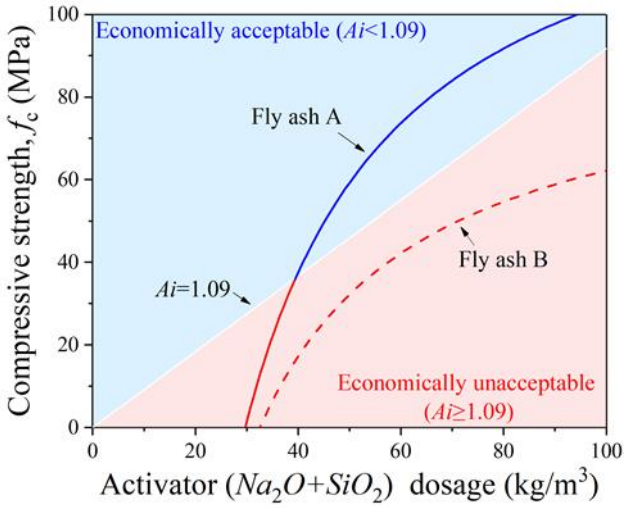

Fig. 11 Activator index (*Ai*)-aided mix design

4. Conclusions

This study presents the first analysis of the CO_2 avoidance cost of geopolymer concrete (GC) to show its economic feasibility. The CO_2 avoidance cost refers to the cost incurred to reduce one metric ton (t) of CO_2 emissions. For GC, it can be determined by comparing its cost and CO_2 emissions with those of blended cement (30% SCMs and 70% OPC) concrete. A total of 486 FAGC mixtures are analyzed in the context of locally-available materials in China. Monte Carlo simulation is used to consider the uncertainty of raw material prices, transport distances, and emission factors.

Given that both capturing CO_2 from cement plants and replacing cement with geopolymer are viable methods for significantly reducing CO_2 emissions, this study compares the CO_2 avoidance cost of GC with that of capturing CO_2 from cement plants to identify the most cost-effective decarbonization technology. The results show that 107 of 486 FAGC mixtures are more cost-effective than capturing CO_2 from cement plants, which has been evaluated to have a CO_2 avoidance cost of 55 USD/tCO_2 in China's demonstration project. Additionally, seven of these mixtures yield negative CO_2 avoidance costs. Capturing CO_2 has always been criticized for being too expensive. These findings suggest that geopolymers may be more expensive than capturing CO_2, highlighting the importance of cost assessment and research aimed at cost reduction.

The results also show that the low CO_2 avoidance cost of FAGC is associated with low activator

dosage and high compressive strength. To quantify this relationship, this study proposes the activator index (*Ai*), the activator dosage ($kg \cdot m^{-3}$) necessary to achieve 1 MPa of compressive strength. The result shows a strong correlation between CO_2 avoidance cost and *Ai*. Specifically, *Ai* < 1.09 $kg \cdot m^{-3}$/MPa and *Ai* < 0.625 $kg \cdot m^{-3}$/MPa correspond to the CO_2 avoidance cost of FAGC lower than 55 USD/tCO_2 and 0. These two *Ai* values also correspond to 51.83% and 59.85% emission reductions of FAGC compared with blended cement concrete. This *Ai*-based criterion can be extended to geopolymer concrete using other precursors, as NaOH and Na_2SiO_3 are the primary activators. It helps identify optimal geopolymer concrete that effectively reduces CO_2 emissions at the lowest possible cost, thereby promoting its commercial application.

5. Future research

At the technical level, FAGC faces some challenges as follows:

- The corrosion behavior of steel bars in FAGC remains uncertain, limiting the application of FAGC in reinforced concrete. A comprehensive study on the corrosion behavior of steel bars in FAGC is imperative. Exploring the combination of FAGC and fiber-reinforced polymer (FRP) bars could offer another solution. In addition, not all concrete is used for reinforced concrete. For other forms of concrete, the excellent chemical and fire resistance of FAGC is beneficial.
- FAGC develops its strength slowly at ambient temperatures and requires slightly elevated temperatures to accelerate its strength development. While this restricts in-situ construction, the application of FAGC in precast components remains viable. Also, the literature suggests that introducing a small amount of calcium by adding slag or cement to FAGC can accelerate the strength development of FAGC at ambient temperatures.

The significant challenge comes from non-technical fields. This paper raises the cost issue of FAGC. Limited cost-effective FAGC mixtures are viable for industrial use. Future research lines include, but are not limited to:

- Developing activators with lower CO_2 emissions and cost than sodium hydroxide or sodium silicate, but with similarly desirable strength development. A potentially feasible idea is using Portland cement to partially replace sodium hydroxide or sodium silicate as the activator. Many

studies reported that adding a small amount of Portland cement can greatly increase the strength of FAGC, especially when cured at ambient temperature [77,94,95,158,159]. Also, a fact is that the emission factor and unit price of Portland cement are lower than sodium hydroxide or sodium silicate, although the CO_2 emissions of CC is higher than GC. Using cement to partially replace sodium hydroxide or sodium silicate has the potential to lower CO_2 emissions and cost while maintaining strength. An in-depth exploration of the performances, mechanisms, CO_2 emissions, and costs associated with the hybrid binder of geopolymer and Portland cement is warranted.

- Developing appropriate water-reducing admixtures for GC to curtail water demand, subsequently reducing activator content and effectively mitigating CO_2 emissions and costs. For CC, adding water-reducing admixtures reduces water demand while maintaining the required flowability. The resulting decrease in concrete porosity reduces the cement content required to achieve the target strength, effectively reducing CO_2 emissions and cost [160]. Unfortunately, the current water-reducing admixtures for CC are not suitable for GC [6].

- Investigating additional sustainability factors for GC beyond CO_2 emissions. For example, the production of CC worldwide contributes approximately 7.8% of NO_X, 4.8% of SO_X, 5.2% of PM10, and 6.4% of PM2.5 [161]. However, there is a lack of study on such air pollutant emissions of GC. Air pollutant emissions cause health damage. Future studies should evaluate the air pollutant emissions of GC.

Data Availability Statement: Data will be made available on request.

Acknowledgments: This work was supported by the National Science Fund for Distinguished Young Scholars (52025081), and Shenzhen Science and Technology Program (GXWD20220817143919002, KQTD20210811090112003, and CJGJZD20220517141800001).

Conflicts of Interest: The authors declare no conflict of interest.

References

[1] Monteiro, P. J., Miller, S. A., & Horvath, A. (2017). Towards sustainable concrete. *Nature Materials*, *16*(7), 698-699.

[2] China Building Materials Federation (CBMF). (2021). Report on Carbon Emissions from China's Building Materials Industry (2020). CBMF, Beijing. (In Chinese)
[3] Scrivener, K. L., John, V. M., & Gartner, E. M. (2018). Eco-efficient cements: Potential economically viable solutions for a low-CO2 cement-based materials industry. *Cement and Concrete Research*, *114*, 2-26.
[4] IEA. (2018). Technology Roadmap - Low-Carbon Transition in the Cement Industry, IEA, Paris. https://www.iea.org/reports/technology-roadmap-low-carbon-transition-in-the-cement-industry
[5] Shi, C., Qu, B., & Provis, J. L. (2019). Recent progress in low-carbon binders. *Cement and Concrete Research*, *122*, 227-250. https://doi.org/10.1016/j.cemconres.2019.05.009
[6] Provis, J. L. (2018). Alkali-activated materials. *Cement and Concrete Research*, *114*, 40-48.
[7] Li, N., Shi, C., Zhang, Z., Wang, H., & Liu, Y. (2019). A review on mixture design methods for geopolymer concrete. *Composites Part B: Engineering*, *178*, 107490. https://doi.org/10.1016/j.compositesb.2019.107490
[8] Habert, G., Miller, S. A., John, V. M., Provis, J. L., Favier, A., Horvath, A., & Scrivener, K. L. (2020). Environmental impacts and decarbonization strategies in the cement and concrete industries. *Nature Reviews Earth & Environment*, *1*(11), 559-573.
[9] Coffetti, D., Crotti, E., Gazzaniga, G., Carrara, M., Pastore, T., & Coppola, L. (2022). Pathways towards sustainable concrete. *Cement and Concrete Research*, *154*, 106718.
[10] Liu, T., Wei, H., Zou, D., Zhou, A., & Jian, H. (2020). Utilization of waste cathode ray tube funnel glass for ultra-high performance concrete. *Journal of Cleaner Production*, *249*, 119333.
[11] Zhou, A., Zhang, W., Wei, H., Liu, T., Zou, D., & Guo, H. (2021). A novel approach for recycling engineering sediment waste as sustainable supplementary cementitious materials. *Resources, Conservation and Recycling*, *167*, 105435.
[12] Wei, H., Zhou, A., Liu, T., Zou, D., & Jian, H. (2020). Dynamic and environmental performance of eco-friendly ultra-high performance concrete containing waste cathode ray tube glass as a substitution of river sand. *Resources, Conservation and Recycling*, *162*, 105021.
[13] Zhou, A., Wei, H., Guo, H., Zhang, W., Liu, T., & Zou, D. (2023). Mechanical performance and environmental potential of concrete with engineering sediment waste for sustainable built environment. *Resources, Conservation and Recycling*, *189*, 106742.
[14] McLellan, B. C., Williams, R. P., Lay, J., van Riessen, A., & Corder, G. D. (2011). Costs and carbon emissions for geopolymer pastes in comparison to ordinary portland cement. *Journal of Cleaner Production*, *19*(9-10), 1080-1090.
[15] Chan, C. C., Thorpe, D., & Islam, M. (2015, December). An evaluation of life long fly ash based geopolymer cement and ordinary Portland cement costs using extended life cycle cost method in Australia. In *2015 IEEE International Conference on Industrial Engineering and Engineering Management (IEEM)* (pp. 52-56).
[16] Rajini, B., Rao, A. V., & Sashidhar, C. (2020). Cost analysis of geopolymer concrete over conventional concrete. *International Journal of Civil Engineering and Technology, 11(02).*
[17] Bajpai, R., Choudhary, K., Srivastava, A., Sangwan, K. S., & Singh, M. (2020). Environmental impact assessment of fly ash and silica fume based geopolymer concrete. *Journal of Cleaner Production, 254,* 120147.
[18] Shobeiri, V., Bennett, B., Xie, T., & Visintin, P. (2021). A comprehensive assessment of the global warming potential of geopolymer concrete. *Journal of Cleaner Production*, *297*, 126669.
[19] Giergiczny, Z. (2019). Fly ash and slag. *Cement and Concrete Research*, *124*, 105826.
[20] Snellings, R., Suraneni, P., & Skibsted, J. (2023). Future and emerging supplementary cementitious materials. *Cement and concrete research*, *171*, 107199.
[21] Di Filippo, J., Karpman, J., & DeShazo, J. R. (2019). The impacts of policies to reduce CO2 emissions within

the concrete supply chain. *Cement and Concrete Composites*, *101*, 67-82.
[22] Schneider, M. (2019). The cement industry on the way to a low-carbon future. *Cement and Concrete Research*, *124*, 105792.
[23] Li, J., Tharakan, P., Macdonald, D., & Liang, X. (2013). Technological, economic and financial prospects of carbon dioxide capture in the cement industry. *Energy Policy*, *61*, 1377-1387.
[24] Zhou, W., Jiang, D., Chen, D., Griffy-Brown, C., Jin, Y., & Zhu, B. (2016). Capturing CO2 from cement plants: A priority for reducing CO2 emissions in China. *Energy*, *106*, 464-474.
[25] Jakobsen, J., Roussanaly, S., & Anantharaman, R. (2017). A techno-economic case study of CO2 capture, transport and storage chain from a cement plant in Norway. *Journal of Cleaner Production*, *144*, 523-539. https://doi.org/10.1016/j.jclepro.2016.12.120
[26] Roussanaly, S. (2019). Calculating CO2 avoidance costs of carbon capture and storage from industry. *Carbon Management*, *10*(1), 105-112.
[27] Conch cement. (2018). Environmental Impact Assessment Report on the CO2 Capture Demonstration Project in Baimashan Cement Plant of Conch Cement. (In Chinese) https://sthjj.wuhu.gov.cn/oldfiles/wuhuoldfiles/UpFiles/annex/003010685/00301068510/20180514_0D639CD63005483FBAD00A591FA341FE.pdf
[28] Hou, H., Su, L., Guo, D., & Xu, H. (2023). Resource utilization of solid waste for the collaborative reduction of pollution and carbon emissions: Case study of fly ash. *Journal of Cleaner Production*, *383*, 135449.
[29] China Concrete and Cement-based Products Association (CCPA). (2021). Industry Development Report of Fly Ash Materials Branch in 2020. (In Chinese)
[30] China Geological Survey. (2011). Lake salt leads the salt industry in China. https://www.cgs.gov.cn/xwl/ddyw/201603/t20160309_277747.html
[31] Wang, F., Wang, S., Li, Z., You, H., Aviso, K. B., Tan, R. R., & Jia, X. (2019). Water footprint sustainability assessment for the chemical sector at the regional level. *Resources, Conservation and Recycling, 142*, 69-77.
[32] Habert, G., & Ouellet-Plamondon, C. (2016). Recent update on the environmental impact of geopolymers. *RILEM technical Letters, 1*, 17-23. https://doi.org/10.21809/rilemtechlett.2016.6
[33] JGJ 55-2011. (2011). Specification for mix proportion design of ordinary concrete. Ministry of Housing and Urban-Rural Development of the People's Republic of China, Beijing. (In Chinese)
[34] Liu, T., Wei, H., Zhou, A., Zou, D., & Jian, H. (2020). Multiscale investigation on tensile properties of ultra-high performance concrete with silane coupling agent modified steel fibers. *Cement and Concrete Composites*, *111*, 103638.
[35] Zhou, A., Yu, Z., Wei, H., Tam, L. H., Liu, T., & Zou, D. (2020). Understanding the toughening mechanism of silane coupling agents in the interfacial bonding in steel fiber-reinforced cementitious composites. *ACS Applied Materials & Interfaces*, *12*(39), 44163-44171.
[36] Wei, H., Liu, T., Zhou, A., Zou, D., & Li, Y. (2023). Toughening static and dynamic damping characteristics of ultra-high performance concrete via interfacial modulation approaches. *Cement and Concrete Composites*, *136*, 104879.
[37] Turner, L. K., & Collins, F. G. (2013). Carbon dioxide equivalent (CO2-e) emissions: A comparison between geopolymer and OPC cement concrete. *Construction and Building Materials*, *43*, 125-130. https://doi.org/10.1016/j.conbuildmat.2013.01.023
[38] Van den Heede, P., & De Belie, N. (2012). Environmental impact and life cycle assessment (LCA) of traditional and 'green' concretes: Literature review and theoretical calculations. *Cement and Concrete Composites*, *34*(4), 431-442.
[39] Yang, K., Song, J., & Song, K. (2013). Assessment of CO2 reduction of alkali-activated concrete. *Journal of*

Cleaner Production, *39*, 265-272.
[40] Salas, D. A., Ramirez, A. D., Ulloa, N., Baykara, H., & Boero, A. J. (2018). Life cycle assessment of geopolymer concrete. *Construction and Building Materials, 190*, 170-177.
[41] Nisbet, M. A., VanGeem, M. G., Gajda, J., & Marceau, M. (2000). Environmental life cycle inventory of portland cement concrete. *PCA R&D Serial*, *28*.
[42] Chen, C., Habert, G., Bouzidi, Y., Jullien, A., & Ventura, A. (2010). LCA allocation procedure used as an incitative method for waste recycling: An application to mineral additions in concrete. *Resources, Conservation and Recycling*, *54*(12), 1231-1240.
[43] China Electricity Council. (2020). Annual Development Report of China's Power Industry in 2020. (In Chinese) http://www.chinapower.com.cn/zx/zxbg/20200615/22414.html
[44] Björklund, A. E. (2002). Survey of approaches to improve reliability in LCA. *The International Journal of Life Cycle Assessment*, *7*, 64-72.
[45] Ravikumar, D., Zhang, D., Keoleian, G., Miller, S., Sick, V., & Li, V. (2021). Carbon dioxide utilization in concrete curing or mixing might not produce a net climate benefit. *Nature communications*, *12*(1), 855.
[46] Assi, L. N., Carter, K., Deaver, E., & Ziehl, P. (2020). Review of availability of source materials for geopolymer/sustainable concrete. *Journal of Cleaner Production*, *263*, 121477.
[47] Wall Material Innovation and Development Center of Inner Mongolia Autonomous Region. (2017). Prominent issues and relevant suggestions regarding the comprehensive utilization of fly ash and the enjoyment of national tax preferential policies in green building materials such as new wall materials. *Wall Materials Innovation & Energy Saving in Buildings, 2017(1)*, 31-32. (in Chinese)
[48] https://price.ccement.com
[49] Ling, W., Xia, Z., & Ruijun, G. (2018). The Recent Research and Market of Concrete Admixture in China. *China Concrete and Cement Products* (07),1-5. (In Chinese) https://doi.org/10.19761/j.1000-4637.2018.07.001
[50] Hong, J., Chen, W., Wang, Y., Xu, C., & Xu, X. (2014). Life cycle assessment of caustic soda production: A case study in China. *Journal of Cleaner Production*, *66*, 113-120.
[51] T/CBMF 27-2018. (2018). Methods and requirements of low-carbon products evaluation for ready-mixed concrete. China Building Materials Federation (CBMF), Beijing. (In Chinese)
[52] Zhang, Z., Zhu, Y., Yang, T., Li, L., Zhu, H., & Wang, H. (2017). Conversion of local industrial wastes into greener cement through geopolymer technology: A case study of high-magnesium nickel slag. *Journal of Cleaner Production*, *141*, 463-471.
[53] RESEARCH INSTITUTE OF HIGHWAY MINISTRY OF TRANSPORT. (2021). Analysis Report on the Operation of China's Road Transportation Industry Based on Big Data (2020). (In Chinese)
[54] GB 175-2007. (2007). Common Portland cement. Standardization Administration of the People's Republic of China, Beijing. (In Chinese)
[55] EN 197-1. (2011). Cement - Part 1: composition, specifications and conformity criteria for common cements. CEN, Brussels.
[56] GB/T 4209-2022. (2022). Sodium silicate for industrial use. Standardization Administration of the People's Republic of China, Beijing. (In Chinese)
[57] Assi, L. N., Deaver, E. (Eddie), ElBatanouny, M. K., & Ziehl, P. (2016). Investigation of early compressive strength of fly ash-based geopolymer concrete. *Construction and Building Materials*, *112*, 807–815.
[58] Shaikh, F. U. A., & Vimonsatit, V. (2015). Compressive strength of fly-ash-based geopolymer concrete at elevated temperatures. *Fire and Materials*, *39*(2), 174–188.
[59] Mehta, A., Siddique, R., Ozbakkaloglu, T., Uddin Ahmed Shaikh, F., & Belarbi, R. (2020). Fly ash and

ground granulated blast furnace slag-based alkali-activated concrete: Mechanical, transport and microstructural properties. *Construction and Building Materials*, *257*, 119548.

[60] Mehta, A., & Siddique, R. (2017). Sulfuric acid resistance of fly ash based geopolymer concrete. *Construction and Building Materials*, *146*, 136–143.

[61] Rai, B., Roy, L. B., & Rajjak, M. (2018). A statistical investigation of different parameters influencing compressive strength of fly ash induced geopolymer concrete. *Structural Concrete*, *19*(5), 1268–1279.

[62] Shi, X. S., Collins, F. G., Zhao, X. L., & Wang, Q. Y. (2012). Mechanical properties and microstructure analysis of fly ash geopolymeric recycled concrete. *Journal of Hazardous Materials*, *237–238*, 20–29.

[63] Zhang, H., Li, L., Sarker, P. K., Long, T., Shi, X., Wang, Q., & Cai, G. (2019). Investigating Various Factors Affecting the Long-Term Compressive Strength of Heat-Cured Fly Ash Geopolymer Concrete and the Use of Orthogonal Experimental Design Method. *International Journal of Concrete Structures and Materials*, *13*(1), 63.

[64] Abdulrahman, H., Muhamad, R., Visintin, P., & Azim Shukri, A. (2022). Mechanical properties and bond stress-slip behaviour of fly ash geopolymer concrete. *Construction and Building Materials*, *327*, 126909.

[65] Nguyen, T. T., Goodier, C. I., & Austin, S. A. (2020). Factors affecting the slump and strength development of geopolymer concrete. *Construction and Building Materials*, *261*, 119945.

[66] Ruengsillapanun, K., Udtaranakron, T., Pulngern, T., Tangchirapat, W., & Jaturapitakkul, C. (2021). Mechanical properties, shrinkage, and heat evolution of alkali activated fly ash concrete. *Construction and Building Materials*, *299*, 123954.

[67] Law, D. W., Adam, A. A., Molyneaux, T. K., Patnaikuni, I., & Wardhono, A. (2015). Long term durability properties of class F fly ash geopolymer concrete. *Materials and Structures*, *48*(3), 721–731.

[68] Gunasekera, C., Setunge, S., & Law, D. W. (2017). Correlations between Mechanical Properties of Low-Calcium Fly Ash Geopolymer Concretes. *Journal of Materials in Civil Engineering*, *29*(9).

[69] Topark-Ngarm, P., Chindaprasirt, P., & Sata, V. (2015). Setting Time, Strength, and Bond of High-Calcium Fly Ash Geopolymer Concrete. *Journal of Materials in Civil Engineering*, *27*(7).

[70] Nuaklong, P., Sata, V., & Chindaprasirt, P. (2016). Influence of recycled aggregate on fly ash geopolymer concrete properties. *Journal of Cleaner Production*, *112*(4), 2300–2307.

[71] Farhan, N. A., Sheikh, M. N., & Hadi, M. N. S. (2019). Investigation of engineering properties of normal and high strength fly ash based geopolymer and alkali-activated slag concrete compared to ordinary Portland cement concrete. *Construction and Building Materials*, *196*, 26–42.

[72] Sarker, P. K. (2011). Bond strength of reinforcing steel embedded in fly ash-based geopolymer concrete. *Materials and Structures*, *44*(5), 1021–1030.

[73] Deb, P. S., Nath, P., & Sarker, P. K. (2014). The effects of ground granulated blast-furnace slag blending with fly ash and activator content on the workability and strength properties of geopolymer concrete cured at ambient temperature. *Materials & Design (1980-2015)*, *62*, 32–39.

[74] Yang, W., Zhu, P., Liu, H., Wang, X., Ge, W., & Hua, M. (2021). Resistance to Sulfuric Acid Corrosion of Geopolymer Concrete Based on Different Binding Materials and Alkali Concentrations. *Materials*, *14*(23), 7109.

[75] Nath, P., & Sarker, P. K. (2014). Effect of GGBFS on setting, workability and early strength properties of fly ash geopolymer concrete cured in ambient condition. *Construction and Building Materials*, *66*, 163–171.

[76] Okoye, F. N., Durgaprasad, J., & Singh, N. B. (2016). Effect of silica fume on the mechanical properties of fly ash based-geopolymer concrete. *Ceramics International*, *42*(2), 3000–3006.

[77] Nath, P., & Sarker, P. K. (2015). Use of OPC to improve setting and early strength properties of low calcium fly ash geopolymer concrete cured at room temperature. *Cement and Concrete Composites*, *55*, 205–214.

[78] Nagajothi, S., & Elavenil, S. (2021). Effect of GGBS Addition on Reactivity and Microstructure Properties of Ambient Cured Fly Ash Based Geopolymer Concrete. *Silicon*, *13*(2), 507–516.
[79] Mehta, A., & Siddique, R. (2017). Strength, permeability and micro-structural characteristics of low-calcium fly ash based geopolymers. *Construction and Building Materials*, *141*, 325–334.
[80] Chindaprasirt, P., & Chalee, W. (2014). Effect of sodium hydroxide concentration on chloride penetration and steel corrosion of fly ash-based geopolymer concrete under marine site. *Construction and Building Materials*, *63*, 303–310.
[81] Gunasekara, C., Dirgantara, R., Law, D. W., & Setunge, S. (2019). Effect of Curing Conditions on Microstructure and Pore-Structure of Brown Coal Fly Ash Geopolymers. *Applied Sciences*, *9*(15), 3138.
[82] Saxena, R., Gupta, T., Sharma, R. K., & Panwar, N. L. (2021). Influence of granite waste on mechanical and durability properties of fly ash-based geopolymer concrete. *Environment, Development and Sustainability*, *23*(12), 17810–17834.
[83] Memon, F. A., Nuruddin, M. F., & Shafiq, N. (2013). Effect of silica fume on the fresh and hardened properties of fly ash-based self-compacting geopolymer concrete. *International Journal of Minerals, Metallurgy, and Materials*, *20*(2), 205–213.
[84] Gomaa, E., Sargon, S., Kashosi, C., Gheni, A., & ElGawady, M. A. (2020). Mechanical Properties of High Early Strength Class C Fly Ash-Based Alkali Activated Concrete. *Transportation Research Record: Journal of the Transportation Research Board*, *2674*(5), 430–443.
[85] Nuruddin, M. F., Demie, S., & Shafiq, N. (2011). Effect of mix composition on workability and compressive strength of self-compacting geopolymer concrete. *Canadian Journal of Civil Engineering*, *38*(11), 1196–1203.
[86] Cui, Y., Gao, K., & Zhang, P. (2020). Experimental and Statistical Study on Mechanical Characteristics of Geopolymer Concrete. *Materials*, *13*(7), 1651.
[87] Olivia, M., & Nikraz, H. (2012). Properties of fly ash geopolymer concrete designed by Taguchi method. *Materials & Design (1980-2015)*, *36*, 191–198.
[88] Verma, M., & Dev, N. (2022). Effect of ground granulated blast furnace slag and fly ash ratio and the curing conditions on the mechanical properties of geopolymer concrete. *Structural Concrete*, *23*(4), 2015–2029.
[89] Zhang, H., Li, L., Long, T., Sarker, P., Shi, X., Cai, G., & Wang, Q. (2019). The Effect of Ordinary Portland Cement Substitution on the Thermal Stability of Geopolymer Concrete. *Materials*, *12*(16), 2501.
[90] Long, T., Wang, Q., Guan, Z., Chen, Y., & Shi, X. (2017). Deterioration and Microstructural Evolution of the Fly Ash Geopolymer Concrete against $MgSO_4$ Solution. *Advances in Materials Science and Engineering*, *2017*, 1–11.
[91] Ivan Diaz-Loya, E., Allouche, E. N., & Vaidya, S. (2011). Mechanical Properties of Fly-Ash-Based Geopolymer Concrete. *ACI MATERIALS JOURNAL*, *108*(3), 300–306.
[92] Cornelis, R., Priyosulityo, H., Satyarno, I., & Rustendi, I. (2022). Effect of the Mortar Volume Ratio on the Mechanical Behavior of Class CI Fly Ash-Based Geopolymer Concrete. *Civil Engineering Journal*, *8*(9), 1920-1935.
[93] Wardhono, A., Law, D., & Molyneaux, T. (2014). The mechanical properties of fly ash geopolymer in long term performance. In *the CIC2014 "concrete innovation conference", Oslo, Norway*.
[94] Shehab, H. K., Eisa, A. S., & Wahba, A. M. (2016). Mechanical properties of fly ash based geopolymer concrete with full and partial cement replacement. *CONSTRUCTION AND BUILDING MATERIALS*, *126*, 560–565.
[95] Hongen, Z., Feng, J., Qingyuan, W., Ling, T., & Xiaoshuang, S. (2017). Influence of Cement on Properties of Fly-Ash-Based Concrete. *ACI Materials Journal*, *114*(5), 745–753.

[96] Pachamuthu, S., & Thangaraju, P. (2017). Effect of incinerated paper sludge ash on fly ash–based geopolymer concrete. *Journal of the Croatian Association of Civil Engineers*, *69*(9), 851–859.
[97] Vora, P. R., & Dave, U. V. (2013). Parametric studies on compressive strength of geopolymer concrete. *Procedia Engineering*, *51*, 210-219.
[98] Zhang, H., Li, L., Yuan, C., Wang, Q., Sarker, P. K., & Shi, X. (2020). Deterioration of ambient-cured and heat-cured fly ash geopolymer concrete by high temperature exposure and prediction of its residual compressive strength. *Construction and Building Materials*, *262*, 120924.
[99] Ahmed, M. F., Nuruddin, M. F., & Shafiq, N. (2011). Compressive strength and workability characteristics of low-calcium fly ash-based self-compacting geopolymer concrete. *International journal of civil and environmental engineering*, *5*(2), 64-70.
[100] Hassan, A., Arif, M., & Shariq, M. (2019). Effect of curing condition on the mechanical properties of fly ash-based geopolymer concrete. *SN Applied Sciences*, *1*(12), 1-9.
[101] Memon, F. A., Nuruddin, M. F., Demie, S., & Shafiq, N. (2011). Effect of curing conditions on strength of fly ash-based self-compacting geopolymer concrete. *International Journal of Civil and Environmental Engineering*, *5*(8), 342-345.
[102] Wallah, S. E. (2010). Creep behaviour of fly ash-based geopolymer concrete. *Civil Engineering Dimension*, *12*(2), 73-78.
[103] Sarker, P. K., Haque, R., & Ramgolam, K. V. (2013). Fracture behaviour of heat cured fly ash based geopolymer concrete. *Materials & Design*, *44*, 580-586.
[104] Shaikh, F. U. A. (2016). Mechanical and durability properties of fly ash geopolymer concrete containing recycled coarse aggregates. *International Journal of Sustainable Built Environment*, *5*(2), 277-287.
[105] Patankar, S. V., Jamkar, S. S., & Ghugal, Y. M. (2013). Effect of water-to-geopolymer binder ratio on the production of fly ash based geopolymer concrete. *Int. J. Adv. Technol. Civ. Eng*, *2*(1), 79-83.
[106] Olivia, M., & Nikraz, H. (2011). Strength and water penetrability of fly ash geopolymer conrete. *Journal of Engineering and Applied Sciences*, *6*(7), 70-78.
[107] Lokuge, W., Wilson, A., Gunasekara, C., Law, D. W., & Setunge, S. (2018). Design of fly ash geopolymer concrete mix proportions using Multivariate Adaptive Regression Spline model. *Construction and Building Materials*, *166*, 472-481.
[108] Gunasekara, C., Atzarakis, P., Lokuge, W., Law, D. W., & Setunge, S. (2021). Novel analytical method for mix design and performance prediction of high calcium fly ash geopolymer concrete. *Polymers*, *13*(6), 900.
[109] Demie, S., Nuruddin, M. F., & Shafiq, N. (2013). Effects of micro-structure characteristics of interfacial transition zone on the compressive strength of self-compacting geopolymer concrete. *Construction and Building Materials*, *41*, 91-98.
[110] Çevik, A., Alzeebaree, R., Humur, G., Niş, A., & Gülşan, M. E. (2018). Effect of nano-silica on the chemical durability and mechanical performance of fly ash based geopolymer concrete. *Ceramics International*, *44*(11), 12253-12264.
[111] Okoye, F. N., Durgaprasad, J., & Singh, N. B. (2015). Mechanical properties of alkali activated flyash/Kaolin based geopolymer concrete. *Construction and Building Materials*, *98*, 685-691.
[112] Jena, S., Panigrahi, R., & Sahu, P. (2019). Mechanical and durability properties of Fly ash Geopolymer concrete with silica fume. *Journal of The Institution of Engineers (India): Series A*, *100*(4), 697-705.
[113] Wang, Y., Hu, S., & He, Z. (2019). Mechanical and fracture properties of fly ash geopolymer concrete addictive with calcium aluminate cement. *Materials*, *12*(18), 2982.
[114] Bellum, R. R., Venkatesh, C., & Madduru, S. R. C. (2021). Influence of red mud on performance enhancement of fly ash-based geopolymer concrete. *Innovative Infrastructure Solutions*, *6*(4), 1-9.

[115]Embong, R., Kusbiantoro, A., Shafiq, N., & Nuruddin, M. F. (2016). Strength and microstructural properties of fly ash based geopolymer concrete containing high-calcium and water-absorptive aggregate. *Journal of cleaner production*, *112*, 816-822.

[116]Pan, Z., Sanjayan, J. G., & Rangan, B. V. (2011). Fracture properties of geopolymer paste and concrete. *Magazine of concrete research*, *63*(10), 763-771.

[117]Kusbiantoro, A., Nuruddin, M. F., Shafiq, N., & Qazi, S. A. (2012). The effect of microwave incinerated rice husk ash on the compressive and bond strength of fly ash based geopolymer concrete. *Construction and Building Materials*, *36*, 695-703.

[118]Joseph, B., & Mathew, G. (2012). Influence of aggregate content on the behavior of fly ash based geopolymer concrete. *Scientia Iranica*, *19*(5), 1188-1194.

[119]Haruna, S., Mohammed, B. S., Wahab, M. M. A., & Liew, M. S. (2020). Effect of paste aggregate ratio and curing methods on the performance of one-part alkali-activated concrete. *Construction and Building Materials*, *261*, 120024.

[120]Kar, A., Ray, I., Unnikrishnan, A., & Halabe, U. B. (2016). Prediction models for compressive strength of concrete with Alkali-activated binders. *COMPUTERS AND CONCRETE*, *17*(4), 523–539.

[121]Aleem, M. A., & Arumairaj, P. D. (2012). Optimum mix for the geopolymer concrete. I*ndian Journal of Science and Technology*, *5*(3), 2299-2301.

[122]Wardhono, A., Gunasekara, C., Law, D. W., & Setunge, S. (2017). Comparison of long term performance between alkali activated slag and fly ash geopolymer concretes. *Construction and Building Materials*, *143*, 272–279.

[123]Luan, C., Shi, X., Zhang, K., Utashev, N., Yang, F., Dai, J., & Wang, Q. (2021). A mix design method of fly ash geopolymer concrete based on factors analysis. *Construction and Building Materials*, *272*, 121612.

[124]Shekhovtsova, J., Kovtun, M., & Kearsley, E. P. (2015). Evaluation of short- and long-term properties of heat-cured alkali-activated fly ash concrete. *Magazine of Concrete Research*, *67*(16), 897–905.

[125]Mortar, N. A. M., Kamarudin, H., Rafiza, R. A., Meor, T. A. F., & Rosnita, M. (2020, May). Compressive Strength of Fly Ash Geopolymer Concrete by Varying Sodium Hydroxide Molarity and Aggregate to Binder Ratio. In *IOP Conference Series: Materials Science and Engineering* (Vol. 864, No. 1, p. 012037). IOP Publishing.

[126]Xie, T., & Ozbakkaloglu, T. (2015). Behavior of low-calcium fly and bottom ash-based geopolymer concrete cured at ambient temperature. *Ceramics International*, *41*(4), 5945–5958.

[127]Al-Azzawi, M., Yu, T., & Hadi, M. N. S. (2018). Factors affecting the bond strength between the fly ash-based geopolymer concrete and steel reinforcement. *Structures*, S2352012418300353.

[128]Hardjito, D., & Rangan, B. V. (2005). Development and properties of low-calcium fly ash-based geopolymer concrete. Available at https://espace.curtin.edu.au/bitstream/handle/20.500.11937/5594/19327_downloaded_stream_419.pdf?sequence=2

[129]DAI Jinxin, SHI Xiaoshuang, WANG Qingyuan, ZHANG Hong'en, LUAN Chenchen, ZHANG Kuanyu, YANG Fuhua. (2021). Effect of Multi-factor on the Compressive Strength of Construction and Demolition Waste Based Geopolymer Concrete. *Materials Reports*, *35*(9): 9077-9082. (In Chinese)

[130]Ali İhsan Çelik, Ahmet Özbayrak, Ahmet Şener, and Mehmet Cemal Acar. Effect of activators in different ratios on compressive strength of geopolymer concrete. *Canadian Journal of Civil Engineering*. *50*(2): 69-79.

[131]Luan, C., Shi, X., Wang, Q., Utashev, N., Tufail, R. F., & Maqsoom, A. (2022). Carbonation performances of steel fiber reinforced geopolymer concrete. *Canadian Journal of Civil Engineering*, *50*(4), 294-305.

[132]Provis, J. L., Arbi, K., Bernal, S. A., Bondar, D., Buchwald, A., Castel, A., ... & Zuo, Y. (2019). RILEM TC 247-DTA round robin test: mix design and reproducibility of compressive strength of alkali-activated concretes. *Materials and Structures*, *52*, 1-13.

[133]Luan, C., Wang, Q., Yang, F., Zhang, K., Utashev, N., Dai, J., & Shi, X. (2021). Practical prediction models of tensile strength and reinforcement-concrete bond strength of low-calcium fly ash geopolymer concrete. *Polymers*, *13*(6), 875.

[134]Tokyay, M., & Özdemir, M. (1997). Specimen shape and size effect on the compressive strength of higher strength concrete. *Cement and Concrete Research*, *27*(8), 1281-1289.

[135]del Viso, J., Carmona, J., & Ruiz, G. (2008). Shape and size effects on the compressive strength of high-strength concrete. *Cement and Concrete Research*, *38*(3), 386-395.

[136]Gopalan, M. K., & Hague, M. N. (1985). Design of flyash concrete. *Cement and concrete research, 15(4)*, 694-702.

[137]Kumar, B., Tike, G. K., & Nanda, P. K. (2007). Evaluation of properties of high-volume fly-ash concrete for pavements. *Journal of Materials in Civil Engineering, 19(10)*, 906-911.

[138]Han, S. H., Kim, J. K., & Park, Y. D. (2003). Prediction of compressive strength of fly ash concrete by new apparent activation energy function. *Cement and Concrete Research, 33(7),* 965-971.

[139]Nath, P., & Sarker, P. (2011). Effect of fly ash on the durability properties of high strength concrete. *Procedia Engineering, 14*, 1149-1156.

[140]Slanička, Š. (1991). The influence of fly ash fineness on the strength of concrete. *Cement and Concrete Research, 21(2-3)*, 285-296.

[141]Oner, A. D. N. A. N., Akyuz, S., & Yildiz, R. (2005). An experimental study on strength development of concrete containing fly ash and optimum usage of fly ash in concrete. *Cement and Concrete Research, 35(6)*, 1165-1171.

[142]Damineli, B. L., Kemeid, F. M., Aguiar, P. S., & John, V. M. (2010). Measuring the eco-efficiency of cement use. *Cement and Concrete Composites*, *32*(8), 555-562.

[143]Talha Junaid, M., Kayali, O., Khennane, A., & Black, J. (2015). A mix design procedure for low calcium alkali activated fly ash-based concretes. *Construction and Building Materials*, *79*, 301-310.

[144]Aughenbaugh, K. L., Williamson, T., & Juenger, M. C. G. (2015). Critical evaluation of strength prediction methods for alkali-activated fly ash. *Materials and Structures*, *48*, 607-620.

[145]Zhang, Z., Provis, J. L., Zou, J., Reid, A., & Wang, H. (2016). Toward an indexing approach to evaluate fly ashes for geopolymer manufacture. *Cement and Concrete Research*, *85*, 163-173.

[146]Kuenzel, C., & Ranjbar, N. (2019). Dissolution mechanism of fly ash to quantify the reactive aluminosilicates in geopolymerisation. *Resources, Conservation and Recycling*, *150*, 104421.

[147]Kumar Mehta, P., & Aietcin, P. C. (1990). Principles underlying production of high-performance concrete. *Cement, concrete and aggregates*, *12*(2), 70-78.

[148]Bharatkumar, B., Narayanan, R., Raghuprasad, B., & Ramachandramurthy, D. (2001). Mix proportioning of high performance concrete. *Cement and Concrete Composites*, *23*(1), 71-80.

[149]Soutsos, M., Boyle, A. P., Vinai, R., Hadjierakleous, A., & Barnett, S. J. (2016). Factors influencing the compressive strength of fly ash based geopolymers. *Construction and Building Materials*, *110*, 355-368.

[150]Ryu, G. S., Lee, Y. B., Koh, K. T., & Chung, Y. S. (2013). The mechanical properties of fly ash-based geopolymer concrete with alkaline activators. *Construction and building materials*, *47*, 409-418.

[151]Zhou, A., Li, K., Liu, T., Zou, D., Peng, X., Lyu, H., ... & Luan, C. (2023). Recycling and optimum utilization of engineering sediment waste into low-carbon geopolymer paste for sustainable infrastructure. *Journal of Cleaner Production*, *383*, 135549.

[152]Leong, H. Y., Ong, D. E. L., Sanjayan, J. G., & Nazari, A. (2016). The effect of different Na2O and K2O ratios of alkali activator on compressive strength of fly ash based-geopolymer. *Construction and Building Materials*, *106*, 500-511.
[153]Wang, W., Fan, C., Wang, B., Zhang, X., & Liu, Z. (2023). Workability, rheology, and geopolymerization of fly ash geopolymer: Role of alkali content, modulus, and water–binder ratio. *Construction and Building Materials*, *367*, 130357.
[154]Somna, K., Jaturapitakkul, C., Kajitvichyanukul, P., & Chindaprasirt, P. (2011). NaOH-activated ground fly ash geopolymer cured at ambient temperature. *Fuel*, *90*(6), 2118-2124.
[155]Gunasekara, C., Setunge, S., & Law, D. W. (2017). Long-term mechanical properties of different fly ash geopolymers. *ACI Structural Journal*, *114*(3), 743.
[156]De Silva, P., Sagoe-Crenstil, K., & Sirivivatnanon, V. (2007). Kinetics of geopolymerization: Role of Al2O3 and SiO2. *Cement and Concrete Research*, *37*(4), 512-518.
[157]Görhan, G., & Kürklü, G. (2014). The influence of the NaOH solution on the properties of the fly ash-based geopolymer mortar cured at different temperatures. *Composites part b: engineering*, *58*, 371-377.
[158]García-Lodeiro, I., Fernández-Jiménez, A., & Palomo, A. (2013). Variation in hybrid cements over time. Alkaline activation of fly ash–portland cement blends. *Cement and concrete research*, *52*, 112-122.
[159]Aliabdo, A. A., Abd Elmoaty, M., & Salem, H. A. (2016). Effect of cement addition, solution resting time and curing characteristics on fly ash based geopolymer concrete performance. *Construction and building materials*, *123*, 581-593.
[160]Cheung, J., Roberts, L., & Liu, J. (2018). Admixtures and sustainability. *Cement and Concrete Research*, *114*, 79-89.
[161]Miller, S. A., & Moore, F. C. (2020). Climate and health damages from global concrete production. *Nature Climate Change*, *10*(5), 439-443.